Alkane dehydrogenation with silica supported platinum and platinum–gold catalysts derived from phosphine ligated precursors

Bert D. Chandler, Leon I. Rubinstein, Louis H. Pignolet [*]

Department of Chemistry, University of Minnesota, Minneapolis, MN 55455, USA

Abstract

In this paper we describe the preparation, catalysis of hexane and propane conversion, and characterization results of several phosphorus containing Pt and Pt–Au catalysts on silica supports. The catalysts were prepared by adsorption from solution of mono- and bi-metallic molecular precursors that are ligated by triphenylphosphine. The effects of phosphorus in the calcined and activated catalysts are much greater than that of gold and lead to remarkable changes in selectivity and stability compared with conventional, non-phosphorus containing Pt/SiO_2 and co-deposited $Pt–Au/SiO_2$ catalysts. All catalysts derived from triphenylphosphine precursors showed high selectivity and activity towards dehydrogenation products. Other reactions, namely cyclization, isomerization and cracking, were severely inhibited. Preliminary results for propane conversion show that phosphorus containing catalysts are excellent catalysts for propane dehydrogenation (90% selectivity to propylene at 35% conversion, 550°C, SV = 0.5 h^{-1}). The phosphorus containing catalysts also have much greater stability on stream than the non-phosphorus containing catalysts. DRIFTS data on adsorbed CO show that the presence of phosphorus in the catalysts has a significant effect on the CO stretching frequency and causes an upward (blue) shift of about 10 cm^{-1}. TPD of adsorbed CO showed that desorption of CO from a phosphorus containing Pt catalyst had a maximum at ca. 140°C while CO desorption from a conventional Pt/SiO_2 catalyst peaked between 240–270°C. These results are consistent with a phosphorus ligand effect on Pt. Preliminary TEM data with a phosphorus containing Pt catalyst showed very small Pt particles estimated to be less than 1 nm. © 1998 Elsevier Science B.V. All rights reserved.

Keywords: Triphenylphosphine precursors; Dehydrogenation products; Cyclization; Isomerization; Cracking

1. Introduction

Supported noble metal catalysts, often with a second metal and other dopants added, are the mainstay of the petrochemical industry and alkane conversion by these catalysts has been widely studied [1,2]. It is well known that the addition of gold can have important effects on the catalytic properties of platinum [3,4]. Since gold by itself is not a catalytically active metal in alkane reforming reactions, the study of Pt–Au alloys offers a good opportunity to test the importance of geometric effects on the catalysis.

The reactivity of Pt–Au catalysts towards *n*-pentane and *n*-hexane conversion has been extensively studied [3–9]. It has been shown that catalysts where platinum is diluted with

---

gold show differences in selectivity [5,6]. Isomerization reactions are favored by the addition of gold to a platinum catalyst when the reaction is conducted at high pressures of H_2 and hexane [6]. Single crystal studies showed that annealing Au on the Pt[111] surface indeed increases both activity and selectivity towards isomerization, while aromatization and hydrogenolysis processes are suppressed [3]. The most recent studies by Sachdev and Schwank showed similar results for SiO_2 supported Pt–Au catalysts [4].

Much of the previous effort in preparing supported mixed-metal Pt–Au catalysts was limited to co-impregnation of Pt and Au salts such as H_2PtCl_6 and $HAuCl_4$ [4,10–12]. Phase separation is a common problem with this method since the Pt–Au alloys that contain between 18% and 97% Pt are thermodynamically unstable. In addition, the presence of Au is known to affect Pt particle size. A different approach is to use organometallic precursors for heterogeneous catalysts, in particular molecular cluster compounds [13–19]. Past studies in this field involved the use of carbonyl clusters as precursors [15,17–21]. In these studies, metal cluster compounds were supported on various oxide supports (silica, alumina, or zeolites) and their carbonyl ligands were removed by heating under vacuum or inert atmosphere. Further studies showed that in some cases the structure of the cluster's metal core remained substantially intact [20].

Unfortunately, there are no known carbonyl clusters that contain both platinum and gold. However, there are many known Pt–Au molecular clusters stabilized by phosphine ligands [22–28]. Several examples of these clusters are $[Pt(AuPPh_3)_8](NO_3)_2$, $[(PPh_3)Pt(AuPPh_3)_6]$ $(NO_3)_2$, and $[Pt(AuPPh_3)_2(PPh_3)_2](NO_3)_2$. These clusters are cationic and have a platinum atom in the center surrounded by a variable number of $AuPPh_3$ and PPh_3 groupings. These Pt–Au clusters contain both Pt–Au and Au–Au bonds. Known triphenylphosphine ligated Pt–Au clusters provide a wide range of Pt:Au ratios, varying from 1:2 to 1:9.

The presence of phosphorus in these potential catalyst precursors may also have substantial effects on the resulting catalysts. There have been very few studies on the effect of phosphorus on alkane conversion catalysis [29]. It is conventional wisdom that phosphorus is a poison for catalysis and should be avoided; however, the addition of phosphorus has been shown to promote HDS and HDN activity for some systems [30–32]. Other suspected poisons such as sulfur have been studied as additives to alkane conversion catalysts [33–35]. These studies indicate that the presence of sulfur, an element not dissimilar to phosphorus, increases both the stability of the catalyst [33,34] and yield of dehydrogenation products while inhibiting often undesirable cracking reactions [35,36]. In general, catalysts modified by sulfur often show superior properties compared to pure platinum systems [2,37–39]. Therefore, it is not surprising that in this study we find similar pronounced effects for phosphorus.

Several phosphine ligated Pt–Au cluster compounds have been supported and thermolized on silica [40–42]. The process of adsorption from solution and the properties of the adsorbed intact clusters, including their thermal activation, were thoroughly studied; however, their catalytic reactivity (H_2–D_2 equilibration and ethylene hydrogenation) has been only briefly investigated [40,41]. Thermolysis experiments showed that the supported clusters $[Pt(AuPPh_3)_8](NO_3)_2$ and $[(PPh_3)Pt(AuPPh_3)_6]$ $(NO_3)_2$ begin decomposing at ca. 200°C under H_2. This decomposition was accompanied by a significant decrease in the rate of H_2–D_2 equilibration. The properties of the catalysts derived from these supported clusters were shown to depend significantly on the treatment conditions [41]. Systems treated only under reductive conditions (H_2) did not chemisorb CO and had very low catalytic activity for H_2–D_2 equilibration and ethylene hydrogenation. However, exposure of the samples to O_2, even at room temperature, resulted in significant increases of both CO uptake and catalytic activity. The data

obtained from ^{31}P CP MAS NMR is consistent with phosphine oxidation upon exposure of the samples to O_2 [41]. Oxygen chemisorption at room temperature indicated that $[Pt(AuPPh_3)_8](NO_3)_2/SiO_2$ takes up ca. 5 mol of O_2 per mol of Pt—consistent with ligand oxidation. Treatment of $[Pt(AuPPh_3)_8]$ $(NO_3)_2/SiO_2$ with O_2 at 230°C resulted in a catalyst with excellent dispersion (0.8 mol CO per mol of Pt by CO chemisorption and metal particles ≤ 1 nm by TEM) and reactivity towards ethylene hydrogenation and $H_2–D_2$ equilibration. Its hydrogenation activity, for example, increased by two orders of magnitude compared to the sample treated only under H_2 [41]. A study on the thermal activation of $[Pt(AuPPh_3)_6(PPh_3)](NO_3)_2/SiO_2$ at 200°C and 400°C under vacuum was recently published by Yuan et al. [42]. Thermolysis at 200°C resulted in a catalyst with poor hydrogenation and H–D exchange activity. EXAFS data suggested that the catalyst they obtained had Pt–P bonds which coincided with poisoning of the catalyst. Thermolysis at 400°C resulted in Pt particles that still showed Pt–P bonds in the EXAFS analysis.

The qualitative picture that emerges from the above studies is that PPh_3 ligated Pt–Au clusters on silica can be calcined under O_2 to give well dispersed and highly active catalysts. Thermolysis under H_2 or vacuum gives poisoned, inactive systems that do not bind CO and show Pt–P bonding by EXAFS. Exposure of these systems to O_2 at room temperature gives active catalysts due to oxidation of the phosphine residues. This qualitative model sets the stage for the current study.

2. Experimental

2.1. Catalyst preparation

Phosphine containing mono- and bi-metallic molecular precursors, $[Pt(AuPPh_3)_8](NO_3)_2$ [43], $Pt(PPh_3)_2O_2$ [44], and $[Pt(AuPPh_3)_2(PPh_3)_2](NO_3)_2$ [45,46], were prepared according to literature procedures and characterized by ^{31}P{^{1}H} NMR, FAB-MS, and UV–visible spectroscopy in solution. Hexachloroplatinic acid, $H_2PtCl_6 \cdot 6H_2O$, was prepared from Pt metal (99.99%) according to a literature procedure [47]. Auric acid $(HAuCl_4 \cdot H_2O)$ was purchased from Strem. Davisil SiO_2 (35–60 mesh, BET surface area 360 m^2 g^{-1}, average pore diameter $= 150$ Å) was washed with high purity millepore distilled and deionized water to remove the fines and dried under vacuum at 120°C for 24 h prior to use. The above precursors were deposited onto the pre-treated SiO_2 support by incipient wetness impregnation and co-impregnation. The solution concentrations were adjusted to give the following metal loadings (weight percents) with catalyst abbreviations: Pt (1% Pt), Au (2% Au), Pt–Au (1% Pt + 2% Au). The phosphine containing precursors $Pt(PPh_3)_2O_2$ and $[Pt(AuPPh_3)_2(PPh_3)_2](NO_3)_2$ spontaneously adsorbed from methylene chloride solution. The appropriate amount (usually 10–20 mg) of the compound was dissolved in 5–10 ml of CH_2Cl_2. The solution was then added to 0.5–1.0 g of dry SiO_2. After swirling for 10–20 min at room temperature the compounds quantitatively adsorbed onto the silica. The impregnated silica was then decanted and dried under vacuum at 50°C for 2 h. $[Pt(AuPPh_3)_8](NO_3)_2$ was similarly supported from methanol solution. In this case, a solution of 10 mg of the cluster in ca. 15 ml MeOH was added to 1 g of silica and swirled for 1 h at room temperature. After that time most (but not all) of the cluster was adsorbed on silica. The solvent was then slowly evaporated under vacuum at room temperature and the sample dried as above. The resulting catalyst loadings and abbreviations are: PtP_2 (1% Pt), $PtAu_2P_4$ (1% Pt + 2% Au), and $PtAu_8P_8$ (0.05% Pt + 0.4% Au).

2.2. Catalyst activation

Catalyst activation, chemisorption measurements, temperature programmed characterizations (TPC), and catalytic investigations were

carried out with the use of an RXM-100 catalyst characterization system purchased from Advanced Scientific Designs. In a typical experiment (except for TPD of CO experiments, vide infra), 50–500 mg of the supported catalyst precursors were loaded into a U-shaped quartz microreactor (i.d. = 11 mm), attached to the RXM-100 system, and heated in the presence of flowing gas as described below. The sample was loaded into the RXM-100 system and purged with O_2 for 5 min at 30°C. The temperature was then ramped 10°C min^{-1} to 300°C and held for 2 h with O_2 flowing at 20 ml min^{-1}. Following the 2 h soak at 300°C, the sample was purged with He flowing at 100 ml min^{-1} while the temperature was ramped 10°C min^{-1} to 200°C. The sample was then reduced at 200°C under flowing H_2 (20 ml min^{-1}) for 1 h. This is the standard catalyst activation procedure used for all experiments unless specifically stated otherwise.

2.3. Gases

Hydrogen, helium, and oxygen were all UHP grade (99.999%) and were used without further purification. Propane (99.5%) was obtained from Scott Specialty Gases. O_2/He and H_2/Ar gas mixtures were purchased in pre-mixed cylinders of UHP grade (99.999%) gases from Linde and were used without further purification.

2.4. Chemisorption experiments

All adsorption isotherms were measured at 20°C over a pressure range of 10–80 Torr. The chemisorption protocol was as follows. Following catalyst pretreatment, samples were cooled 10°C min^{-1} to 135°C and evacuated for 20 min. The samples were then cooled to room temperature under high vacuum and the furnace was replaced with a water bath. CO chemisorption was then measured using the two isotherm method. In each chemisorption experiment, two gas uptakes were measured. Between the two measurements, the sample was evacuated at

20°C for 10 min. In CO chemisorption experiments, the dispersion ($Pt_{surface}$/Pt_{total}) is equal to the ratio of adsorbed CO to total platinum atoms (CO/Pt_{total}) calculated from the irreversible CO uptake at 60 Torr on catalyst samples using the adsorption stoichiometry CO:Pt as 1:1 [48]. However, it has been reported that for very small Pt particles the CO:Pt ratio can exceed unity [1]. Accuracy in the determination of CO/Pt_{total} values was ± 0.02. CO chemisorptions were reproducible after CO desorption under vacuum at 300°C. The blank silica support showed no irreversible CO uptake.

2.5. Temperature programmed characterization

Temperature programmed oxidation (TPO) was performed on supported (non-activated) precursors. The samples were loaded into the quartz microreactor described above and heated at a constant rate (usually 10°C min^{-1}) under flow of 3% O_2/He. For CO temperature programmed desorption experiments, large sample sizes (ca. 1.7 g) were used in order to reduce experimental error. These samples were placed in a larger quartz reactor (inner volume ca. 2 ml) and treated according to the standard catalyst activation protocol. The samples were then treated under H_2 at 400°C for 1 h and evacuated at room temperature. Previously used samples were re-reduced under H_2 at 400°C for 1 h and evacuated at room temperature. After CO chemisorption, helium was flowed through the sample for about 30 min in order to let the TCD output stabilize. The sample was then heated at a constant rate (usually 10°C min^{-1}) and the effluent gas was monitored by a TCD detector and mass spectrometer. The mass spectrometer used was a Leybold Inficon Quadrex 200 Residual Gas Analyzer.

2.6. Diffuse Reflectance Infrared Fourier-Transform Spectroscopy (DRIFTS)

DRIFTS studies were conducted with a Magna 750 FTIR system (Nicolet) using a

DRIFTS cell (SpectraTech) equipped with a SpectraTech accessory that allows in situ treatments with different gasses at temperatures up to 900°C. OMNIC software was used for data processing. A liquid nitrogen cooled MCT detector was used for data collection. The interferograms typically consisted of 256 or 512 scans and the spectra were collected with a 2 cm^{-1} resolution. Spectra were obtained in the absorbance format.

2.6.1. DRIFTS of adsorbed CO

The silica supported precursors were pretreated by the usual activation protocol. In some cases they had been previously used in standard hexane conversion experiments (vide infra). The samples were then finely ground (important) and placed into the DRIFTS cell where they were re-reduced under a flow of H_2 at 200°C. The spectra of the samples were collected using the spectrum of air as a background. The samples were then treated with carbon monoxide at room temperature under atmospheric pressure by flowing CO through the cell for 1 min followed by flushing the cell with nitrogen for 2 min. The spectra were then collected. In order to best observe the peaks corresponding to bound CO, the spectra collected before the CO treatment were subtracted from the spectra after the CO treatment.

2.6.2. DRIFTS of adsorbed pyridine

All samples were first treated with O_2 in the RXM-100 reactor at 300°C for 2 h. Spectra of adsorbed pyridine were collected after reductive treatment at 400°C under H_2 for 2 h in the DRIFTS cell. In these experiments the IR spectra were first collected on freshly reduced samples without pyridine added. Then pyridine vapor in N_2 was introduced into the DRIFTS cell with an air-tight syringe and pyridine was allowed to adsorb on the catalyst for approximately 20 min. The DRIFT spectra were then collected and the previously obtained spectra of the freshly reduced samples were subtracted.

2.7. Transmission Electron Microscopy (TEM) and Energy Dispersive Spectroscopy (EDS)

TEM imaging was carried out with use of a Philips CM30 transmission electron microscope equipped with a LaB_6 filament and operated at 300 keV. Images were recorded on film and transferred to a digital format using a flatbed scanner. Samples were prepared by grinding the catalyst with an agate mortar and pestle and sonicating the powder in hexanes for 2 h. This suspension was then dripped from a Pasteur pipette onto a holey carbon grid (Ted Pella) and allowed to dry. EDS were obtained from an attached EDAX PV9900 energy dispersive spectrometer equipped with an ultrathin window and operating with a resolution of about 165 eV.

2.8. Hexane conversion

A saturated hexane in hydrogen gas stream was produced by bubbling hydrogen through a gas dispersion frit immersed in hexane (99 + % hexane, purchased from Aldrich) in a 250 ml round bottom flask sealed with a rubber septum. The round bottom flask was submerged in an ice bath to maintain a hydrogen:hexane ratio of 16:1 (corresponds to a partial pressure of hexane = 49 Torr). The gas mixture was fed directly to the RXM-100 reaction manifold where it subsequently flowed over the catalyst bed. The catalysis runs were all conducted at 400°C. The weight hourly space velocity (WHSV = (g hexane fed)(g Pt)$^{-1}$(h^{-1})) of hexane was typically between 0–2000 h^{-1}. Reaction products were analyzed on stream via gas chromatography (Hewlett-Packard 5890A gas chromatograph operated with FID detection). Separation was achieved with use of a 30-ft SP-1700 Coated 80/100 Chromosorb P AW packed column (Supelco) operated at 90°C and column head pressure of 100 psi. Products were identified by calibrating peak retention times with known hydrocarbons. The products were classified into four types: cracking (formation of C_1–C_5 hydrocarbons), isomerization (2-methyl- and 3-

methylpentane), hexenes, and cyclization (methylcyclopentane). Yields of products were measured in mass percent. Blank runs with plain SiO_2 and Au did not show significant activity under reaction conditions.

2.9. Propane conversion

Propane dehydrogenation experiments were carried out at 550°C with use of a micro flow reactor. A pure propane flow was introduced through a mass flow controller and the space velocities $(SV = (g \text{ propane fed})(g \text{ catalyst})^{-1}(h^{-1}))$ typically ranged from 0.2 to 2 h^{-1}. Products were analyzed on line by gas chromatography.

2.10. Toluene hydrogenation

Toluene hydrogenation experiments were carried out with a toluene–H_2 gas mixture generated in a similar fashion as in the hexane conversion catalysis study. Hydrogen was bubbled through liquid toluene (Mallinckrodt, HPLC grade) maintained at room temperature (toluene partial pressure = 22 Torr). The gas mixture was flowed through the catalyst bed maintained at 60°C. The methylcyclohexane and toluene were detected and quantified by gas chromatography.

3. Results

3.1. The catalysts

A series of silica supported platinum catalysts was prepared in order to study the effects of gold, phosphorus, and precursor type on selectivity, activity, and catalyst structure. Catalysts derived from monometallic non-phosphorus containing precursors were prepared from hexachloroplatinic and auric acids by wetness co-impregnation from water. The phosphorus containing monometallic precursor used was

$Pt(PPh_3)_2O_2$. Catalysts derived from bimetallic phosphorus containing precursors were prepared from the cluster compounds $[Pt(AuPPh_3)_8]$ $(NO_3)_2$ and $[Pt(AuPPh_3)_2(PPh_3)_2](NO_3)_2$. Silica was chosen as the support because it is relatively inert [2]. All phosphorus containing compounds, both mono- and bi-metallic, spontaneously adsorb on silica from methylene chloride or methanol solution. The clusters remain intact on the support prior to calcination [40,41]. The supported materials were treated by initial oxidation under flowing O_2 at 300°C for 2 h followed by a reduction under flowing hydrogen at 200°C for 1 h. Activation conditions were chosen to be as mild as possible based on temperature programmed oxidation and reduction experiments. Temperature programmed oxidation for all supported phosphine precursors indicated that ligand oxidation occurs primarily between 250°C and 300°C. Prior work also showed that an oxidation step was necessary to give active catalysts [40,41]. Elemental analysis and confirmed the majority of the phosphorus from the precursors remained on the support after activation and after catalysis. The catalyst abbreviations with indicated metal loadings (wt.% on SiO_2) used in this study are given in Section 2.

3.2. Hexane conversion

The hexane conversion reaction was chosen to evaluate the performance of the catalysts because a wide array of products can be formed (vide infra). Platinum–gold catalysts prepared from monometallic, non-phosphorus containing precursors have also been extensively studied for this reaction [3,4,49,50]. All experiments were run with the use of a micro flow reactor thermostated at 400°C with a 1:16 hexane:H_2 flow mixture. WHSV's ranged approximately from 10–2000 h^{-1} to achieve hexane conversions between 2 and 25%. Space velocities are for total Pt in the catalyst and are not corrected for Pt dispersion (vide infra). The contact times $(T = (\text{catalyst volume})/(\text{volumetric flow of}$

hexane + H_2)) reported are proportional to the inverse space velocity (WHSV)$^{-1}$. The major product classifications used hereafter are: cracking (C_1–C_5 hydrocarbons), isomerization (2-methylpentane and 3-methylpentane), hexenes, cyclization (methylcyclopentane and cyclohexane), and benzene. Selectivities of different catalysts at low conversion (ca. 2%) are shown in Table 1. It is apparent from this table that the presence of phosphorus in the catalyst precursor is the primary factor in determining the selectivity of the catalyst. Whenever phosphines are present in the molecular precursor, the catalyst selectivity shifts almost exclusively towards the production of hexenes.

The Pt and Pt–Au catalysts are not selective for any specific product. Fig. 1A shows the selectivity vs. conversion profile for the Pt catalyst. The Pt–Au catalyst shows a similar selectivity vs. conversion dependence to that of Pt. Since the effects of phosphorus were so much greater than that of gold, we will not discuss the differences between Pt and Pt–Au in this paper. At very low conversions (< ca. 2%), hexenes are the major product. As conversion increases, the dehydrogenation selectivity rapidly decreases while the selectivity towards isomerization, cyclization, and cracking increases. For these catalysts, methylcyclopentane and methylpentanes are the major products of catalysis at conversions above ca. 10%. These observations are consistent with literature data [4] and with proposed models for dehydrogenation and skeletal isomerization of hydrocarbons by metals [1,51,52].

Table 1
Selectivities (%) for hexane conversion at low overall conversion (ca. 2%)[a]

Catalyst	Cracking	Isomerization	Cyclization	Dehydrogenation
Pt	14	12	37	35
Pt–Au	8	15	46	31
PtP_2	2	0	0	98
$PtAu_2P_4$	6	3	0	91
$PtAu_8P_8$	9	3	0	89

[a]See text for product classifications and catalyst abbreviations.
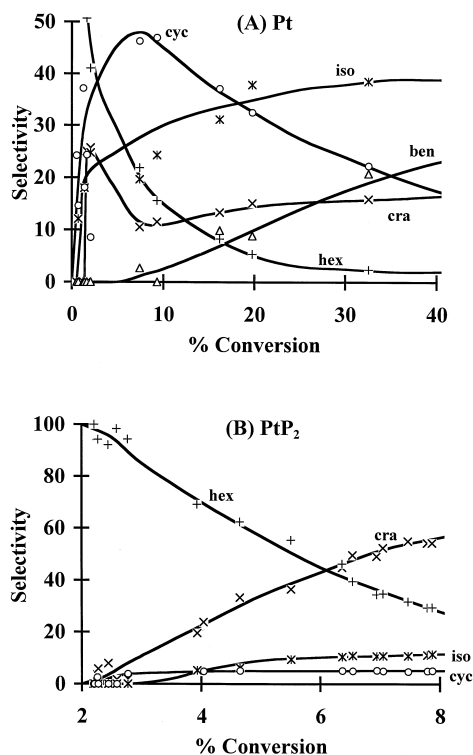

Fig. 1. Product selectivity dependence on conversion of hexane for the catalysts Pt (A) and PtP_2 (B). The products are designated as follows: hex = hexenes, iso = isomerization, cyc = cyclization, cra = cracking, and ben = benzene. No benzene was observed for PtP_2 (B) and the lines are drawn only to help see the trends.

When phosphorus is present in the catalyst precursor, however, there is a dramatic shift in observable activity and in product selectivities (Table 1, Fig. 1). For all three phosphorus containing catalysts, (PtP_2, $PtAu_2P_4$, and $PtAu_8P_8$), we were unable to achieve conversions above 10%, even at very low space velocities (i.e., long contact times). At higher space velocities, the catalysts maintained conversions of ca. 2%. Conversions of less than 2% could only be achieved with WHSVs = 2–5000 ($T = 0.5$–0.05 s). In this lowest conversion regime, selectivity towards dehydrogenation products was routinely at or near 100%.

As space velocities were drastically decreased to increase conversion, some production of cracking, isomerization, and cyclization products was observed. The decrease in selectivity

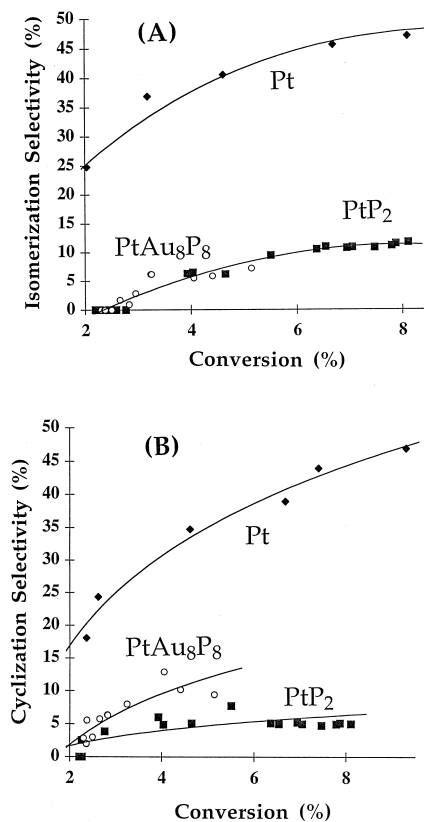Fig. 4. Stability on stream for the catalysts $PtAu_8P_8$ and Pt during hexane conversion at 400°C.

Fig. 2. Dependence of cyclization (A) and isomerization (B) selectivities on conversion. Selectivities are expressed as a percent of products vs. total hexane conversion to all products for the catalysts Pt, PtP_2, and $PtAu_8P_8$.

towards hexene production at higher conversions follows a similar trend as the Pt catalyst; however, only selectivity towards cracking in-
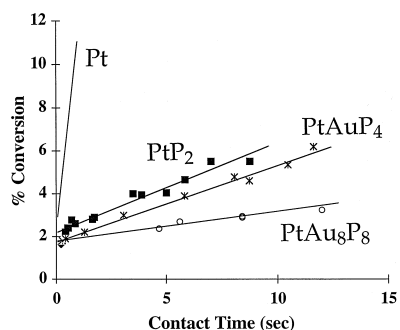

Fig. 3. Plots of total hexane conversion (%) vs. contact time (s) for the phosphorus containing catalysts PtP_2, $PtAu_2P_4$, and $PtAu_8P_8$. The line for the Pt catalyst is shown for comparison purposes and to illustrate its much faster rate of conversion.
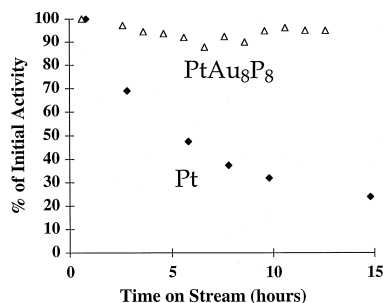
creases greatly (Fig. 1). As shown in Fig. 2, there is little production of cyclization or isomerization products by the phosphorus containing catalysts. It is worth noting that there is a linear relationship between percent conversion and contact time for these catalysts, shown in Fig. 3. The slopes of these percent conversion vs. contact time plots ($T > 0.5$ s) have small values compared to Pt and they all have non-zero intercepts of ca. 2% conversion.

The presence of phosphorus in the catalyst also greatly affects catalyst longevity. The phosphorus containing catalysts show much greater stability on stream under the hexane conversion reaction conditions than the non-phosphorus containing catalysts. Fig. 4 shows a comparison of stabilities on stream for $PtAu_8P_8$ and Pt. In the course of 16 h, the activity of the Pt catalyst decreases by about 75% while the activity of $PtAu_8P_8$ remains nearly constant.

3.3. Propane dehydrogenation

Since the phosphorus containing catalysts showed high activity and selectivity for the dehydrogenation of hexane, some experiments were run with propane in order to evaluate a more practical reaction. All experiments were run in a micro flow reactor at 550°C with a pure propane flow. A plot of propylene selectivity vs. total percent conversion for several of the catalysts is shown in Fig. 5. The phosphorus containing catalysts show much better selectivity for propylene production, typically around 90%
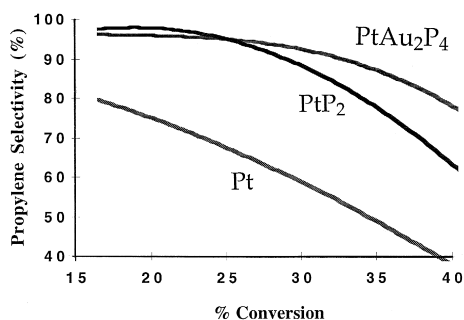
Fig. 5. Selectivity of propane dehydrogenation to propylene vs. total conversion for the catalysts Pt, PtP_2, and $PtAu_2P_4$.

at 35% conversion. Propylene yields ranged from 5–50 g propylene per gram Pt per hour, depending on catalyst, space velocity, etc. The Pt catalyst gave only about 50% selectivity at 35% conversion and became inactive due to coking in less than 1 h. The phosphorus containing catalysts do partially deactivate to ca. 70% of the initial activity after several hours on stream but can be regenerated with oxygen treatment.

3.4. Catalyst characterization; CO chemisorption

All catalysts were subjected to CO chemisorption measurements in order to evaluate the percent of total Pt available for CO bonding. The room temperature irreversible uptakes of these catalysts are shown in Table 2.

All of the samples calcined under O_2 showed similar CO uptake, except Au which did not chemisorb CO and was inactive in all catalysis reactions studied. These results agree qualitatively with DRIFTS data (vide infra) that indicates CO coverage for the Pt containing catalysts is similar. The CO uptake for Pt also agrees very well with the TEM data (vide infra) which shows an average Pt particle size of 3 nm, corresponding to a Pt dispersion of about 45% [1,53]. These values are in good agreement with the literature data for Pt on silica [54].

3.5. DRIFTS

The results of DRIFTS experiments of adsorbed CO are shown in Fig. 6 and the CO stretch absorption maxima are given in Table 2. The Pt catalyst has a CO stretch at 2066 cm^{-1}, in agreement with some literature values [55]. Surprisingly, addition of gold does not greatly alter the CO stretching frequency. A lowering (red shift) of only 4 cm^{-1} was observed with Pt–Au while some papers report shifts of up to 10–15 cm^{-1} upon Au alloying [3,56,57]. This difference might be explained by the use of different supports, pre-treatment and sample preparation conditions, and spectroscopic technique. Previous studies used transmission spectroscopy whereas we used the diffuse reflectance technique. It is well known that the
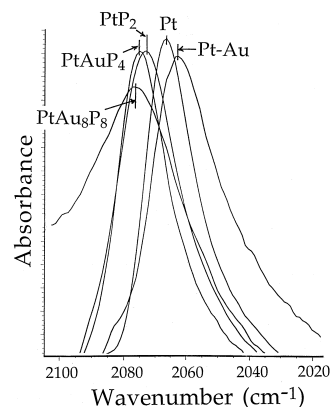
Table 2
Irreversible chemisorption of CO and adsorbed CO stretching frequency data for the catalysts[a]

Catalyst	CO uptake (% of total Pt)[b]	CO stretch (cm^{-1})[c]
Pt	44	2066
Au	~ 0	–
Pt–Au	32	2062
$PtAu_2P_4$	20	2077
PtP_2	48	2073
$PtAu_8P_8$	60	2076

[a]All measurements were made at room temperature.
[b]Activation under O_2 at 300°C for 2 h followed by H_2 at 200°C for 1 h.
[c]Measured by DRIFTS as described in Section 2. Values did not significantly change after hexane conversion catalysis.

Fig. 6. DRIFTS of CO chemisorbed on Pt, Pt–Au, PtP_2, $PtAu_2P_4$, and $PtAu_8P_8$.

CO stretching frequency is very sensitive to variables in sample preparation technique [55,57–60].

The presence of phosphorus in the catalysts has a significant effect on the CO stretching frequency and causes an upward (blue) shift of about 10 cm^{-1}. The CO stretching frequency of these catalysts did not change after hexane conversion catalysis. Absence of such change implies that the catalyst structure and composition does not change significantly under catalytic conditions. This result is consistent with elemental analysis data that show the phosphorus content in the catalysts did not decrease after overnight catalysis. The phosphorus content of the oxidatively calcined catalysts after overnight hexane conversion catalysis remained greater than 75% (elemental analysis data) of the original phosphorus adsorbed. DRIFTS spectra contained no peaks due to C–H and C=C stretches in the phenyl groups [61], indicating oxidation of the organic portions of the ligands. These results agree with the results of elemental analysis indicating that the carbon content of the catalysts decreases sharply after oxidative treatment at 300°C.

DRIFTS experiments were also carried out on catalyst samples that were treated with pyridine. In these experiments the IR stretches of the six-member heterocyclic ring observed in the 1450–1650 cm^{-1} region were monitored to evaluate the acidity of the catalyst. These stretching frequencies are very sensitive to protonation (formation of PyH^+, Brønsted acidity) and ligation with the support (formation of PyL, Lewis acidity) [62]. The pyridine treated Pt catalyst has the exact same features as the spectrum of pyridine adsorbed on pure silica support. PtP_2 has an additional peak at 1491 cm^{-1}; however, the intensity for this peak is very low.

3.6. Temperature programmed desorption (TPD) of CO

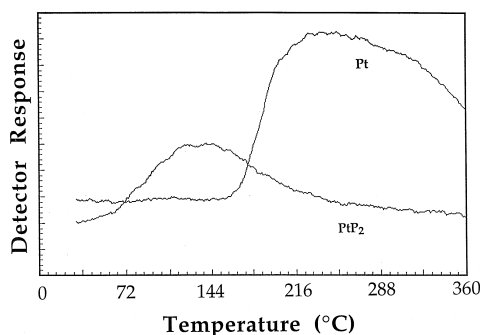TPD experiments were conducted with the Pt and PtP_2 catalysts in order to evaluate the effect

Fig. 7. Temperature programmed desorption (TPD) CO profiles for Pt and PtP_2 recorded with use of the thermal conductivity detector.

of phosphorus on CO desorption. As shown by Herz et al. [63], TPD of CO is extremely sensitive to experimental variables such as the flow rate of the inert gas and rate of temperature increase. In order to obtain comparable TPD results, experimental conditions used for both catalysts were carefully reproduced (see Section 2 for details). The desorbed gases were monitored by the thermal conductivity detector (TCD) and by a mass spectrometer. A significant difference in the temperature of CO desorption for these two catalysts was observed as shown in Fig. 7. Desorption of CO from PtP_2 had a maximum at ca. 140°C while CO desorption from Pt peaked between 240–270°C. Moreover, desorption from PtP_2 was very clean, giving only CO. For Pt, the desorption products contained a significant amount of CO_2. The higher temperature of desorption with Pt probably results in reaction with residual water or surface OH groups or possibly CO disproportionation into CO_2 and C [64].

3.7. Transmission Electron Microscopy (TEM)

Preliminary TEM analysis has been carried out on the Pt and PtP_2 catalysts. For Pt, the average particle size (3 nm) and size distribution are similar to literature values [4]. The average particle size is also consistent with CO chemisorption data previously described. The results for PtP_2 indicate very small Pt particles

at the resolution limit of our instrument. Energy dispersive spectroscopy (EDS) and electron energy loss spectroscopy (EELS) of this sample confirmed the presence of Pt and P. We estimate the average particle size to be less than 1 nm and particles of about 0.5 nm are observable. This experiment needs to be repeated on a higher resolution instrument; however, it is clear that the use of the triphenylphosphine containing precursor for this catalyst results in much smaller Pt particles.

4. Discussion

It is apparent that the primary factor in determining the properties of the resulting catalyst is the presence or absence of phosphines in the catalyst precursor. We believe that all the data can be best explained by a model in which the phosphine residues act as selective poisons for cracking, isomerization, and cyclization reactions. The dehydrogenation of hexane is not poisoned relative to the Pt catalyst; however, high conversions can not be achieved because this reaction is at equilibrium and therefore is not limited kinetically. This conclusion about the paraffin/olefin equilibrium holds for both phosphorus and non-phosphorus containing catalysts and is supported by thermodynamic data. At 400°C, $\Delta G°$ for hexane dehydrogenation to hexenes is 22.45 kJ mol^{-1} [65] which corresponds to 1.95% conversion of hexane to hexenes at equilibrium under the reaction conditions. This value is very close to the intercepts of the plots in Fig. 3. Additionally, the absolute activity (percent conversion) of PtAu$_8$P$_8$ is very close to that of PtP$_2$ and PtAu$_2$P$_4$, despite a 20-fold difference in Pt loading (Pt loading of PtAu$_8$P$_8$ is only 0.05%). At very short contact times and low conversions, the activities of the phosphorus containing catalysts are also comparable to that of the Pt catalyst. This conclusion about the thermodynamic control of dehydrogenation is also consistent with the previously described model and with the observations that

dehydrogenation is faster than other process that occur in reforming [1].

For the non-phosphorus containing catalysts Pt and Pt–Au, other processes such as cyclizations are also fast; thus, olefin selectivities are lower than for phosphorus containing systems in which all the secondary reactions are strongly inhibited. These are the reactions that can lead to high hexane conversion since they are thermodynamically neutral or favorable. When phosphorus is present in the catalyst, however, these secondary processes are severely poisoned. The dependence of selectivity on percent conversion for the phosphorus containing catalyst PtP$_2$ is shown in Fig. 1B; the data for the other phosphorus containing catalysts are similar. Because of the hexane/hexenes equilibrium, the absolute production of olefins remains stable while production of cracking products increases with increasing conversion, resulting in increased selectivity towards the latter. The isomerization and cyclization reactions are the most severely poisoned. A comparison of the selectivity for cyclization and isomerization for the non-phosphorus containing Pt catalyst to PtP$_2$ and PtAu$_8$P$_8$ is shown in Fig. 2. It is clear that the presence of phosphorus in the catalyst severely inhibits these reactions.

The phosphorus containing catalysts have much lower observable activity for total hexane conversion than the non-phosphorus containing catalysts. Even at 1% conversion, the rate of the back reaction producing hexane from hexenes is significant; hence, conversion data does not accurately represent an intrinsic reaction rate. However, we wish to emphasize that the dehydrogenation reaction is NOT poisoned by the presence of phosphorus. Combining the conversion, selectivity, and space velocity data, Fig. 8A shows the plots of olefin yield (olefin yield = (conversion)(selectivity)(WHSV)) vs. the weight hourly space velocity for Pt and PtP$_2$. The plots for the two catalysts are virtually identical: olefin yield increases linearly with space velocity over a very wide range of space velocities (three orders of magnitude). This
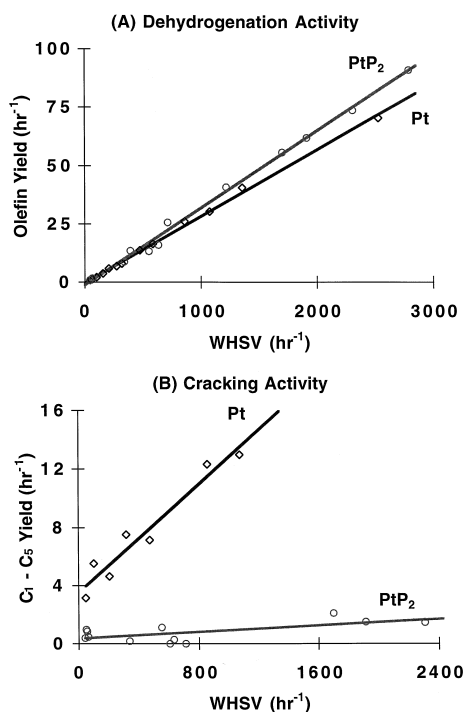
Fig. 8. Dependence of olefin yield (A) and $C_1–C_5$ (cracking products) yield (B) on WHSV for the catalysts Pt and PtP_2.

It is possible that during oxidative activation of the phosphorus containing catalysts some surface acidic sites were produced. This acidity might be responsible for some of the observed cracking activity for phosphorus containing catalysts (vide supra) [1]. DRIFTS experiments with adsorbed pyridine indicate an additional small peak at 1491 cm^{-1}, a frequency assignable to PyH$^+$ and identical to the Brønsted acidity peak for pyridine on alumina [62,67]. The intensity of the peak is very low; however, it is plausible that oxidized phosphorus on the support introduces some weak Brønsted acidity to the catalyst. For some of these catalysts, we observe some production of methane whereas we do not observe methane produced by the Pt catalyst. Beyond the production of small quantities of methane; however, we see no major differences in cracking product distributions that might indicate a drastic change in the mechanism of C–C bond scission when phosphorus is present.

Selective poisoning by phosphorus is also consistent with the enhanced longevity observed with the phosphorus containing catalysts for both the hexane conversion (Fig. 4) and propane dehydrogenation reactions. Because the phospine derived systems have lower rates of cracking and dehydrocyclization, they may be less susceptible to some coking processes. Indeed, this was the rationale for examining the propane dehydrogenation reaction. Under propane flow we do observe the formation of coke; however, the phosphine derived catalysts are much more resistant to deactivation than the Pt catalyst. In addition, the selectivities and conversions of these catalysts for propane dehydrogenation are comparable to many patented industrial catalysts for this reaction [33,34,68–74]. The reaction conditions have not been significantly varied and the system has not been tuned, so it is probable that the performance of the phosphorus containing catalysts can be improved. Work in progress is directed at optimizing the catalyst (e.g., metal loading, support) and conditions of reaction.

would be expected for a process operating at equilibrium and indicates that the dehydrogenation process is similar for the two catalysts. Moreover, all the catalysts studied are likely to have similar rates of dehydrogenation and hydrogenation. This is supported by experiments showing that the catalysts Pt and PtP_2 have similar rates for toluene hydrogenation to methylcyclohexane [66].

Despite the increased selectivity towards cracking products at higher conversion, cracking reactions are inhibited when the phosphorus is present in the catalyst. The cracking selectivity increases at higher conversion for PtP_2 (Fig. 1B) because it is the dominant secondary reaction available. This becomes apparent by comparing the cracking yields (computed in the analogous fashion to the olefin yield) of Pt and PtP_2 vs. space velocity, shown in Fig. 8B. This plot clearly shows that cracking reactions are significantly faster for the Pt catalyst.

CO chemisorption experiments with the Pt catalyst indicate good agreement between dispersion measured by this method and particle size measured with TEM (vide supra). Chemisorption data obtained for bimetallic compounds are more difficult to interpret since they do not necessarily provide direct information about particle size. For example, a highly dispersed catalyst where a non-chemisorbing metal is predominantly on the surface would have a very low chemisorption. Carbon monoxide is also known to restructure an alloy surface and bring the metal that binds CO more strongly (Pt in this case) to the surface [56]. However, the bimetallic catalysts in this study have reasonable CO chemisorption values that are generally consistent with TEM results (vide infra) and with previous measurements of H_2 and O_2 chemisorption [40]. The CO chemisorption measurement for $PtAu_8P_8$ showed a Langmuir isotherm pattern of CO uptake suggesting that CO coverage increases with increasing CO pressure. Chemisorption on Pt resulted in a linear CO uptake indicating that the Pt surface is saturated with CO even at low CO pressure. This result implies possible restructuring of the $PtAu_8P_8$ catalyst during the experiment, a conclusion that agrees with the previously reported data [75]. Chemisorption data for the phosphorus containing catalyst PtP_2 may also be difficult to relate to Pt particle size since bound phosphorus may be blocking some of the surface Pt sites. TEM results on PtP_2 show very small Pt particles between 0.5 and 1 nm suggesting that this may indeed be the case [76].

The DRIFTS results summarized in Table 2 also indicate intimate interaction between phosphorus and platinum in the phosphine derived catalysts. Two explanations have been forwarded for CO stretching frequency shifts in alloyed and doped Pt catalysts—geometric and electronic effects [77]. Typically, dilution of the CO binding metal with an inert material would reduce CO dipole–dipole coupling thus causing a red shift in the CO stretching frequency. This explanation has been predominant in under-

standing of red shifts in the CO stretch in bimetallic catalysts. However, since a blue shift is observed in the phosphorus containing catalysts, this explanation is not applicable to these systems. Other possibilities involve an electronic 'ligand' effect of the bound phosphorus on platinum or a geometric compression of the adlayers of CO due to the presence of phosphorus [58,60]. According to the electronic argument, bound phosphorus would reduce electron density on Pt thus diminishing $d\pi$–$p\pi$ backbonding and strengthening the C–O bond. The geometric argument suggests that phosphorus causes Pt to form small 'islands' where CO ligands are closer together than on a normal Pt surface. The proximity of CO ligands would then increase the dipole–dipole coupling and shift the IR observable symmetric stretch upwards [2,58,60]. Evidence for direct Pt–P bonding was recently reported in an EXAFS study on a similar silica supported, triphenylphosphine Pt–Au cluster derived system [42]. An electronic 'ligand' explanation is consistent with the experimental data since an electronegative phosphorus would make platinum less electron rich, thus reducing back-bonding to CO and increasing the CO stretching frequency. A geometric compression of the CO adlayers also remains a possibility. Such an explanation has been used in the case of oxygen on supported Pt catalysts [56,58]. Finally, one also cannot rule out the possibility that the use of triphenylphosphine ligated precursors results in Pt particles with a different morphology, thus causing a shift in the adsorbed CO stretch.

The CO TPD experiments argue in favor of a phosphorus ligand effect on Pt as opposed to a geometric effect. The difference of over 100°C in the temperatures in CO desorption from Pt and PtP_2 is quite remarkable. A lower CO desorption temperature for the phosphorus containing PtP_2 is also consistent with the DRIFTS data described above, since a blue shift in the CO stretching frequency on PtP_2 might indicate a weakened interaction between CO and the metal. A study by Bain et al. found that catalyst

poisoning by H_2S drastically reduced the temperature of CO desorption from Pt/Al_2O_3 [64]. This observation agrees well with the similarities in catalytic behavior between sulfur and phosphorus containing systems (vide infra).

5. Conclusions

Catalysts prepared from triphenylphosphine containing precursors retain most of the phosphorus after oxidative activation. All of the phosphorus containing catalysts irreversibly take up a significant amount of CO. The presence of phosphorus has a marked effect on the properties of these systems. The catalysts PtP_2, $PtAu_2P_4$, and $PtAu_8P_8$ exhibit a similar blue shift in the stretching frequency of chemisorbed CO compared to the Pt and Pt–Au catalysts. This shift is consistent with CO TPD data which indicates that CO is bound much weaker to Pt in the phosphorus containing catalysts. These observations implicate an electronic ligand effect of phosphorus on Pt. Oxidized phosphorus on the support also causes a small increase in the catalysts Brønsted acidity as shown by the DRIFTS of adsorbed pyridine. TEM data indicate that the PtP_2 catalyst has very small Pt particles (< 1 nm) compared with the Pt catalyst (ca. 3 nm).

The presence of phosphorus has a dramatic effect on hexane conversion reactivity compared with the non-phosphorus containing catalysts. All catalysts derived from triphenylphosphine precursors showed high selectivity towards dehydrogenation products. Importantly, the dehydrogenation rate was fast enough for the reaction to reach thermodynamic equilibrium at high flow rates. Other reactions, namely cyclization, isomerization, and cracking, were severely inhibited. At higher conversions selectivity towards cracking activity increased for the phosphorus containing catalysts; however, the absolute rate of cracking was much slower than with the non-phosphorus containing Pt catalyst. Cracking reactions might be promoted by a small number of Brønsted acid sites present in the phosphine derived systems; however the cracked product distributions are similar for phosphorus and non-phosphorus containing catalysts. The high rate of dehydrogenation suggests that catalysts with very low Pt loading will show similar dehydrogenation performance while all the other reactions will be inhibited even more. This feature makes these triphenylphosphine derived catalysts potentially valuable for selective dehydrogenation of lighter alkanes to alkenes. The presence of phosphorus in PtP_2 did not greatly inhibit the rate of toluene hydrogenation compared with the Pt catalyst. This result indicates that the presence of phosphorus does not inhibit structure insensitive hydrogenation, consistent with the observation of rapid dehydrogenation. Preliminary results for propane conversion show that phosphorus containing catalysts such as PtP_2 are excellent catalysts for propane dehydrogenation, comparable to patented industrial catalysts for this process [33,34,68–74].

The effect of phosphorus on catalyst properties was found to be similar in some ways to the reported effects of sulfur [2,37–39]. Both dopants inhibit structure sensitive cracking and isomerization while promoting dehydrogenation. Also, similar to sulfur, phosphorus has a positive effect on catalyst stability. Detailed studies on sulfur effects have not been published; however, results reported here indicate that the beneficial effects of phosphorus are probably more pronounced. More studies need to be conducted to elucidate the form of the phosphorus in these catalysts and to try to understand its dramatic effects on the catalytic properties.

References

[1] B.C. Gates, J.R. Katzer, G.C.A. Schuit, Chemistry of Catalytic Processes, McGraw-Hill, New York, 1979.

[2] V. Ponec, G.C. Bond, Catalysis by Metals and Alloys, in: B. Delmon, J.T. Yates (Eds.), Studies in Surface Science and Catalysis, Vol. 95, Elsevier, Amsterdam, 1995.

[3] J.W.A. Sachtler, G.A. Somorjai, J. Catal. 81 (1983) 77.

[4] A. Sachdev, J. Schwank, J. Catal. 120 (1989) 353.

[5] J.R.H. van Shaik, R.P. Dessing, V. Ponec, J. Catal. 38 (1975) 273.

[6] H.C. de Jongste, F.J. Kuijers, V. Ponec, in: B. Delmon, P.A. Jacobs, G. Poncelet (Eds.), Proc. Int. Symp. Heterogeneous Catalysis, Brussels, 1975, Elsevier, Amsterdam, 1976, p. 207.

[7] R.P. Dessing, V. Ponec, React. Kinet. Catal. Lett. 5 (1976) 251.

[8] A.F. Kane, J.K.A. Clarke, J. Chem. Soc. Faraday Trans. I 76 (1980) 1640.

[9] J.K.A. Clarke, I. Manninger, T. Baird, J. Catal. 54 (1978) 230.

[10] J.M. Dumas, C. Geron, H. Hadrane, P. Marecot, J. Barbier, J. Mol. Catal. 77 (1992) 87.

[11] J.C. Menezo, M.F. Denanot, S. Peyrovi, J. Barbier, Appl. Catal. 15 (1985) 353.

[12] J. Barbier, P. Marecot, G. Mabilon, D. Durant, M. Prigent, French Patent 90/15,750, 1990.

[13] B.C. Gates, L. Guczi, H. Knozinger, in: B. Delmon, J.T. Yates (Eds.), Metal Clusters in Catalysis, Studies in Surface Science and Catalysis, Vol. 29, Elsevier, Amsterdam, 1986.

[14] S. Kawi, O. Alexeev, M. Shelef, B.C. Gates, J. Phys. Chem. 99 (1995) 6926.

[15] R. Ugo, C. Dossi, R. Psaro, J. Mol. Catal. A 107 (1996) 13.

[16] Y. Iwasawa, M. Yamada, J.C.S. Chem. Commun. (1985) 675.

[17] J.R. Anderson, D.E. Mainwaring, J. Catal. 35 (1974) 162.

[18] J.R. Anderson, P.S. Elmes, R.F. Howe, D.E. Mainwaring, J. Catal. 50 (1977) 508.

[19] F.S. Xiao, M. Ichikawa, Cuihua Xuebao 14 (1993) 87.

[20] O. Alexeev, S. Kawi, M. Shelef, B.C. Gates, J. Phys. Chem. 100 (1996) 253.

[21] P. Braunstein, J. Rose, in: I. Bernal (Ed.), Stereochemistry of Organometallic and Inorganic Compounds, Vol. 3, Elsevier, Amsterdam, 1988, p. 3.

[22] L.H. Pignolet, M.A. Aubart, K.L. Craighead, R.A.T. Gould, D.A. Krogstad, J.S. Wiley, Coord. Chem. Rev. 143 (1995) 219.

[23] L.H. Pignolet, D.A. Krogstad, in: H. Schmidbauer (Ed.), Gold: Progress in Chemistry, Biochemistry and Technology, Wiley, Chichester, England, 1998, in press.

[24] L.H. Pignolet, in: R.D. Adams, F.A. Cotton (Eds.), Catalysis by Di- and Polynuclear Metal Cluster Complexes, VCH Publishers, New York, 1997, in press.

[25] A.M. Mueting, B.D. Alexander, P.D. Boyle, A.L. Casalnuovo, L.N. Ito, L.H. Pignolet, Inorg. Synth. 28 (1992) 279.

[26] L.I. Rubinstein, L.H. Pignolet, Inorg. Chem. 35 (1996) 6755.

[27] A.M. Mueting, W. Bos, B.D. Alexander, P.D. Boyle, J.A. Casalnuovo, S. Balaban, L.N. Ito, S.M. Johnson, L.H. Pignolet, New J. Chem. 12 (1988) 505.

[28] J.J. Steggerda, Comments Inorg. Chem. 11 (1991) 113.

[29] S. Muller, E. Newson, 11th Int. Congress on Catalysis, Heterogenized Platinum Clusters as Dehydrogenation Catalysts, Baltimore, MD, 1996, Abstract Po-073.

[30] S.M.A.M. Bouwens, J.P.R. Vissers, V.H.J. de Beer, R. Prins, J. Catal. 112 (1988) 401.

[31] W.R.A.M. Robinson, J.N.M. van Gestel, T.I. Korányi, S. Eijsbouts, A.M. van der Kraan, J.A.R. van Veen, V.H.J. de Beer, J. Catal. 161 (1996) 539.

[32] S. Eijsbouts, J.N.M. van Gestel, E.M. van Oers, R. Prins, J.A.R. van Veen, V.H.J. de Beer, Appl. Catal. A 119 (1994) 293.

[33] S.A.I. Barri, US Patent 4,795,732, 1989.

[34] S.A.I. Barri, R. Tahir, US Patent 5,126,502, 1992.

[35] D.E. Resasco, B.K. Marcus, C.S. Huang, V.A. Durante, J. Catal. 146 (1994) 40.

[36] H. Wang, G.L. Haller, Bimetallic Pt–Sn/L–Zeolite Catalysts Studied with Chemisorption and X-ray Absorption Spectroscopy, 15th Meeting of the North Am. Catal. Soc., Abstract, Chicago, IL, 1997, p. 73.

[37] G. Leclercq, H. Charcosset, R. Maurel, C. Betizeau, C. Bolivar, R. Frety, D. Jaunay, H. Mendez, L. Tournayan, Bull. Soc. Chim. Belg. 88 (1979) 577.

[38] R.W. Rice, K. Lu, J. Catal. 77 (1982) 104.

[39] Y.J. Huang, S.C. Fung, W.E. Gates, G.B. McVicker, J. Catal. 118 (1989) 192.

[40] I.V.G. Graf, PhD Thesis, Univ. of Minnesota, Minneapolis, 1996.

[41] I.V.G. Graf, J.W. Bacon, M.E. Curley, L.N. Ito, L.H. Pignolet, Inorg. Chem. 35 (1996) 689.

[42] Y. Yuan, K. Asakura, H. Wan, K. Tsai, Y. Iwasawa, Chem. Lett., 1996, p. 129.

[43] R.P.F. Kanters, J.J. Bour, P.P.J. Schlebos, W.P. Bosman, H. Behm, J.J. Steggerda, L.N. Ito, L.H. Pignolet, Inorg. Chem. 28 (1989) 2591.

[44] C.D. Cook, G.S. Jauhal, J. Am. Chem. Soc. 90 (1968) 1464.

[45] L.N. Ito, A.M.P. Felicissimo, L.H. Pignolet, Inorg. Chem. 30 (1991) 387.

[46] P.D. Boyle, B.J. Johnson, B.D. Alexander, J.A. Casalnuovo, P.R. Gannon, S.M. Johnson, E.A. Larka, A.M. Mueting, L.H. Pignolet, Inorg. Chem. 26 (1987) 1346.

[47] D.C. Giedt, C.J. Nyman, Inorg. Synth. 8 (1966) 239.

[48] J.L. Lemaitre, P.G. Menon, F. Delannay, in: F. Delannay (Ed.), Chemical Industry Series: Characterization of Heterogeneous Catalysts, Vol. 15, Marcel Dekker, New York, 1984, p. 316.

[49] K. Balakrishnan, J. Schwank, J. Catal. 132 (1991) 451.

[50] J. Schwank, K. Balakrishnan, A. Sachdev, in: L. Guczi, F. Solymosi, P. Tetenyi (Eds.), New Frontiers in Catalysis: Proc. 10th Int. Congress on Catalysis, Budapest, Vol. 1, Elsevier, Amsterdam, 1993, p. 905.

[51] F.G. Gault, Adv. Catal. 30 (1981) 1.
[52] Z. Paál, Adv. Catal. 29 (1980) 273.
[53] O.M. Poltorak, V.S. Boronin, Russ. J. Phys. Chem. 40 (1966) 1436.
[54] C.R. Adams, H.A. Benesi, R.M. Curtis, R.G. Meisenheimer, J. Catal. 1 (1962) 336.
[55] E.P. Kundig, D. McIntosh, M. Moskovits, G.A. Ozin, J. Am. Chem. Soc. 95 (1973) 7234.
[56] K. Balakrishnan, A. Sachdev, J. Schwank, J. Catal. 121 (1990) 441.
[57] Y. Soma-Noto, W.M.H. Sachtler, J. Catal. 34 (1974) 162.
[58] J. Sarkany, M. Bartok, R.D. Gonzalez, J. Catal. 81 (1983) 347.
[59] M. Primet, J.M. Basset, M.V. Mathieu, M. Prettre, J. Catal. 29 (1973) 213.
[60] F. Stoop, F.J.C.M. Toolenaar, V. Ponec, J. Catal. 73 (1982) 50.
[61] J. Pouchet, The Aldrich Library of Infrared Spectra, Aldrich Chemical, Milwaukee, WI, 1981.
[62] E.P. Parry, J. Catal. 2 (1963) 371.
[63] R.K. Herz, J.B. Kiela, S.P. Marin, J. Catal. 73 (1982) 66.
[64] F.T. Bain, S.D. Jackson, S.J. Thomson, G. Webb, E. Willocks, J. Chem. Soc., Faraday I 72 (1976) 2516.
[65] J.H. Sinfelt, in: T.B. Drew, J.W. Hoopes, T. Vermeulen (Eds.), Advances in Chemical Engineering, Vol. 5, Academic Press, New York, 1964, p. 37.
[66] B.D. Chandler, A. Schabel, L.H. Pignolet, Alkane conversion and arene hydrogenation by platinum-based catalysts prepared from supported molecular precursors: effects of phosphorus and gold, 17th Conference on Catalysis of Organic Reactions, New Orleans, LA, 1998, manuscript submitted for publication.
[67] T. Kawai, K.M. Jiang, T. Ishikawa, J. Catal. 159 (1996) 288.
[68] P.C. Aben, J.C. Platteeuw, B. Stouthamer, Rec. Trav. Chim. 89 (1970) 449.
[69] B.V. Vora, P.R. Pujado, R.F. Anderson, Energy Progress 6 (1986) 171.
[70] F.M. Brinkmeyer, D.F. Rohr, M.E. Olbrich, L.E. Drehman, Oil Gas J. 28 (1983) 75.
[71] B.D. Alexander, G.A. Huff, US Patent 5,453,558, 1995.
[72] R.D. Cortright, J.A. Dumesic, J. Catal. 148 (1994) 771.
[73] S.J. Miller, US Patent 4,727,216, 1988.
[74] D.L. McKay, M.E. Olbrich, US Patent 4,902,849, 1990.
[75] R. Bouwman, W.M.H. Sachtler, J. Catal. 19 (1970) 127.
[76] L.I. Rubinstein, PhD Thesis, Chap. 1, 1997.
[77] F.J.C.M. Toolenaar, F. Stoop, V. Ponec, J. Catal. 82 (1983) 1.